Seagrass mapping using Landsat-8 satellite images in Tanjung Merah waters, Bitung City, North Sulawesi

[1]Jesica O. Patty, [2]Billy T. Wagey, [3]Ferdinand F. Tilaar, [3]Lawrence J. L. Lumingas, [2]Calvyn F. A. Sondakh, [4]Suzanne Undap, [2]Deiske Sumilat

[1] Postgraduate Aquatic Science Study Program, Faculty of Fisheries and Marine Science, Sam Ratulangi University, Manado-95115, Indonesia; [2] Marine Science Study Program, Faculty of Fisheries and Marine Science, Sam Ratulangi University, Manado-95115, Indonesia; [3] Aquatic Resource Management Study Program, Faculty of Fisheries and Marine Science, Sam Ratulangi University, Manado-95115, Indonesia; [4] Aquaculture Study Program, Faculty of Fisheries and Marine Science, Sam Ratulangi University, Manado-95115, Indonesia. Corresponding author: B. T. Wagey, billywagey@unsrat.ac.id

Abstract. Seagrass is a resource that plays an important role in the ecosystem. However, human activities such as overfishing, coastal development, and pollution pose as major threats to the marine environment, especially on seagrasses. Mapping technology by utilizing remote sensing produces new information needed so that it can provide benefits in effective planning and implementation to protect coastal resources. The purpose of this study is to determine the distribution and condition of seagrass and to verify the feasibility of using habitat cover map technology in Tanjung Merah waters using maximum likelihood (ML) approach. The results showed that seagrass cover in the coastal waters of Tanjung Merah is 52.81 ha, categorized as having dense cover (51-75%). This is a stark contrast to other locations, such as the Tanjung Merah and Mayat coastal areas, probably due to the prevalent destructive human activities in these areas.
Key Words: mapping, marine, Northern Sulawesi, seagrass beds.

Introduction. The importance of seagrass ecosystem in maintaining coastal ecosystems and hosting marine biodiversity (Topouzelis et al 2018) and habitat for fish and vulnerable species is well-established (Bujang et al 2006; Blandon & zu Ermgassen 2014). Due to their ecological benefits, seagrasses also support the economy of local communities in coastal areas (Hossain et al 2015). In coastal areas, the population of seagrass beds is very vulnerable to natural physical disturbances, especially in Indonesia (Fonseca et al 2002). Seagrasses are also threatened due to anthropogenic impacts (Green & Short 2003; Lotze et al 2006; Orth et al 2006).

For conservation purposes, it is vital to quantify the extent of the remaining seagrass beds in a particular region. This is highly feasible especially with technological advances in such as spatial approach using satellite image data (Cao et al 2011). Landsat 8 is the latest generation of the Landsat program (Suyarso 2019). The use of Landsat 8 image remote sensing techniques can provide benefits in planning and implementing effective ways to protect coastal resources, namely seagrass in Tanjung Merah waters in combination with data on the distribution and condition of seagrass beds.

Material and Method

Description of the study site. The study was conducted in Tanjung Merah coastal waters, Bitung City, North Sulawesi (Figure 1) from September to October 2020. Three sampling locations were established: RCTI (Resort Ciptaan Tuhan yang Indah), Tanjung Merah, and Mayat (Table 1).

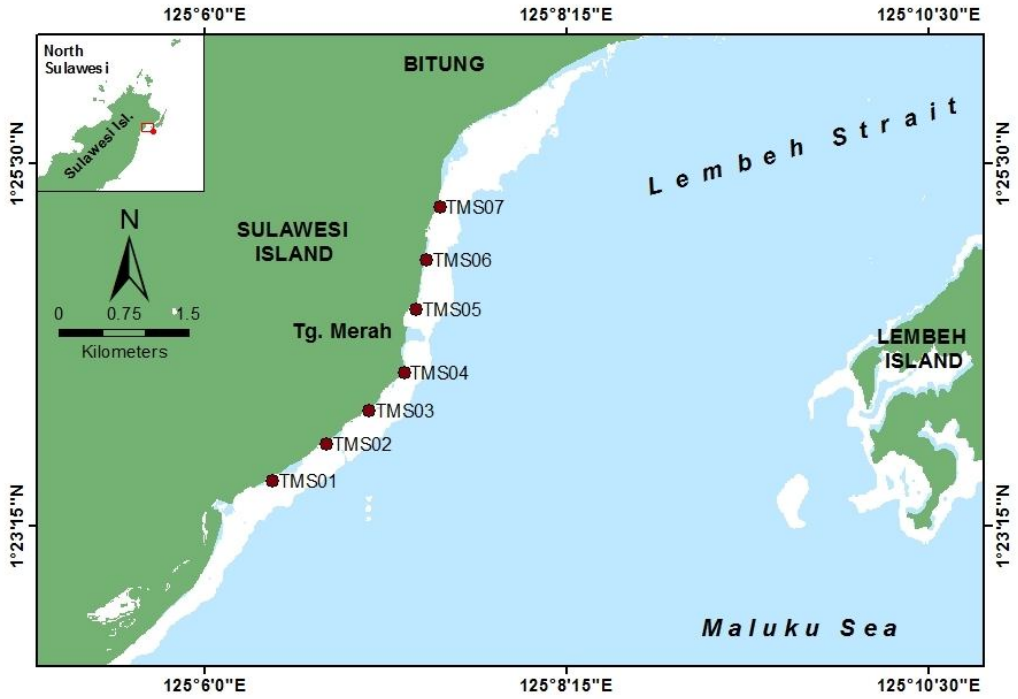

Figure 1. Location map of Tanjung Merah waters, Bitung City, North Sulawesi.

Table 1

Location and position of stations in seagrass survey

Location code	*Station*	*North Latitude*	*East Longitude*	*Locality*
RCTI	TMS01	1.39205	125.10701	Turtle Pier
	TMS02	1.39594	125.11263	RCTI Beach Tourism
Tanjung	TMS03	1.39932	125.11705	Tanjung Merah Boat Mooring
Merah	TMS04	1.40324	125.12065	Tanjung Merah
	TMS05	1.40981	125.12189	PT. Nutrindo
Mayat	TMS06	1.41495	125.12295	Mayat Beach Tourism
	TMS07	1.42038	125.12433	Mayat Boat Mooring

Field experiment. In producing maps with high accuracy, it is necessary to take sample points or training areas or test areas (Region of Interest) as input for this classification. Training represents each class based on the homogeneity of shallow seabed habitats. Groundtruth was done manually by using a boat only in the water area of the research location and moved from one point to another while collecting data. Groundtruth directly observes the cover of the dominant object, then it was recorded along with position of the sample point using GPS. This method is called the Stop and Go method (BIG 2014).

Data collection was carried out on three transects in each station by drawing transect lines perpendiculary from the coastline with a length of 100 meters each. The distance between transects is 50 meters. Quadrats (50 cm x 50 cm) were placed on the right side of each transect on a distance of 10 meters between two consecutive quadrats (Rahmawati et al 2014).

Seagrass analysis. In each frame the composition of seagrass species, dominance, mean, percentage cover and average seagrass cover per station value were recorded:
- calculating the seagrass cover in one frame:

$$\text{Seagrass cover (\%)} = \frac{\text{Total seagrass cover for frame}}{\text{Number of frame}} \times 100$$

- calculating the average seagrass cover per station:

$$\text{Mean (\%)} = \frac{\text{Total seagrass cover for all transects}}{\text{Total of frame for all transects}} \times 100$$

- calculating the average dominance of seagrass species at one station:

$$\text{Mean (\%)} = \frac{\text{Total domination of every type of seagrass in the whole frame}}{\text{Total of frames across the transects}} \times 100$$

- calculating the average seagrass cover per location:

$$\text{Mean (\%)} = \frac{\text{Total average value of seagrass cover for all stations in one location}}{\text{Total of stations in one location}} \times 100$$

Analysis of seagrass condition data based on the coverage was classified into four categories, namely: rare (0-25%), moderate (26-50%), dense (51-75%) and very dense (76-100%) (Rahmawati et al 2014).

Image analysis. This analysis used ENVI 5.3 and ArGIS software. This research consisted of three stages, namely image analysis, Groundtruth and image interpretation test. The methodological framework for image data analysis consists of: image data collection, image data processing, image analysis, and accuracy testing. The wavelength channels used in mapping are blue channel (band 2), green channel (band 3), red channel (band 4) and near infrared channel (band 5). The visible spectrum used in this study is a true color composite or a combination of blue, green and red channels called RGB 432. Its function can distinguish objects only in shallow water (Campbell 1996). Near infrared channels were used to limit land and water areas (USGS 2016).

Image dataset. This research was based on Landsat-8 (Operational Land Imager; OLI) satellite imagery recorded on 08 March 2020 with ID LC08_L1TP_111059_20200308_20200314_01_T1 on Path: 111 and Row: 059. These images were explored and downloaded from the United States Geological Survey (USGS) Earth Explorer web service (http://earthexplorer.usgs.gov).

Image data processing. Image data processing consists of radiometric correction, sunglint correction, water column correction and accuracy assessment. Radiometric correction used an equation (USGS 2015) which is called top of atmosphere (ToA) (Table 2):

$$\rho\lambda = (M\rho * Qcal + A\rho)/\sin(\theta)$$

where: $\rho\lambda$ = top of atmosphere (ToA) reflectance;
$M\rho$ = 'REFLECTANCE_MULT_BAND_n' per band;
$A\rho$ = 'REFLECTANCE_ADD_BAND_n' per band;
Qcal = digital number value;
θ = sun-elevation angle value.

Sunglint correction used de-glint equation (Hedley et al 2005):

$$bij' = bij-(aij).(bNIR-bNIRmin)$$

where: bij' = image of the derivative of bij;
aij = slope regression of the sample of bij;
bNIRmin = minimum sample value of bNIR.

Water column correction used the equation "depth invariant index" (Lyzenga 1978):

$$Y = \ln(Li) - (ki/kj)*\ln(Lj)$$

$$[ki/kj = a + \sqrt{(a2+1)} \text{ and } a = (var_i-var_j/2*covar_{ij})]$$

where: Y = extraction of water base information;
Li = reflectance value in band i;
Lj = reflectance value in the band j;
Ki/kj = ratio of attenuation coefficient in band i and band j pair;
a = slope of k_i/k_j;

i = number of reflectance band i;
j = number of reflectance band j;
Var_i = variant i;
Var_j = variant j;
$Covar_{ij}$ = covariant i and j.

Table 2

Parameters Mρ, Aρ, Qcal, and θ for each band on the Landsat-8 OLI recording (March 08, 2020)

Parameter	*Band 1*	*Band 2*	*Band 3*	*Band 4*	*Band 5*	*Band 6*	*Band 7*	*Band 8*
Mρ	0.00002	0.00002	0.00002	0.00002	0.00002	0.00002	0.00002	0.00002
Aρ	-0.1000	-0.1000	-0.1000	-0.1000	-0.1000	-0.1000	-0.1000	-0.1000
Qcal	b1	b2	b3	b4	b5	b6	b7	b8
θSE	59.97194966 (sinθSE) = 0.86578051462							

Accuracy test used an accuracy matrix table (Table 3). Kappa accuracy or Kappa coefficient using an equation (Green et al 2000) is a discrete multivariate way of calculating the classification accuracy value of the confusion matrix and has a kappa coefficient which has a range of possibilities from 0 to 1. The limit of the acceptable accuracy value for shallow water base habitat maps based on SNI 7716 (2011) concerning mapping of shallow seabed habitats is 60% (Lillesand et al 2008; Congalton & Green 2009).

Table 3

Accuracy matrix table

		Data sample (j)		*Total (ni+)*
Citra Classification (i)	n_{11}	n_{12}	n_{1k}	n_{1+}
	n_{21}	n_{22}	n_{2k}	n_{2+}
	n_{k1}	n_{k2}	n_{kk}	n_{k+}
Total n_{+j}	n_{+1}	n_{+2}	n+k	N

Source: Cangalton & Green (2009).

Overall accuracy = $\frac{\sum_{i=1}^{k} n_{ii}}{n} X\ 100$

Producer accuracy j = $\frac{n_{jj}}{n_{+j}} X\ 100$

User accuracy i = $\frac{n_{ii}}{n_{i+}} X\ 100$

Results and Discussion. Manually selected satellite imagery contains: cloud-free imagery, calm seas such as low or steady wind speed, and absence of major oceanographic phenomena such as fronts, eddies (Topouzelis et al 2018). This Landsat 8 image has corrected the geometry with the WGS'84 datum using the Universal Transverse Mercator (UTM) coordinate system.

The main problem in the initial remote sensing process was the presence of clouds and fog which can affect image quality and can remove the information needed in the remote sensing image that will be used (Kustiyo & Hayati 2016). Radiometric correction was carried out to overcome the disturbance which causes the digital number (DN) value not to be "0" in the darkest objects such as cloud shadows and deep sea. To overcome this, image calibration is carried out, namely changing the pixel value to a reflectant value using an algorithm through the ToA equation (USGS 2015).

The principle of passive (sunlight) or active (sensor) remote sensing undergoes two times atmospheric scattering and underwater attenuation in each medium Veettil et al (2020). The image enhancement used for mapping shallow seabed habitats is sun glint

correction and water column correction, by taking advantage of the effects of atmospheric disturbances and attenuation coefficients (Giardino et al 2019).

The uncorrected Glint image has a high pixel value due to the effect of reflection by sunlight on the sea surface which forms a perfect reverse angle to the sensor so that objects under the water column cannot be seen or blurred. This interference is overcome by utilizing the near infrared light (NIR) band, according to the de-glint equation (Hedley et al 2005). A linear regression equation was used between the near infrared (NIR) ray band as a reference (x) and the visible light band (RGB) corrected by (y). Sampling for pixel glint uses the ROI (Region of Interest) facility in calm (dark) deep sea waters without glint disturbances and waters that have maximum glint disturbances and small glint disturbances. The minimum value of the near infrared band (bNIR) sample obtained from the glinting sample is 1.1813 (NIRmin = 1.1813). Based on the minimum sample value of bNIR (NIRmin = 1.1813) and the regression plot (Figure 2), a de-glint derivative image is obtained (Table 4).

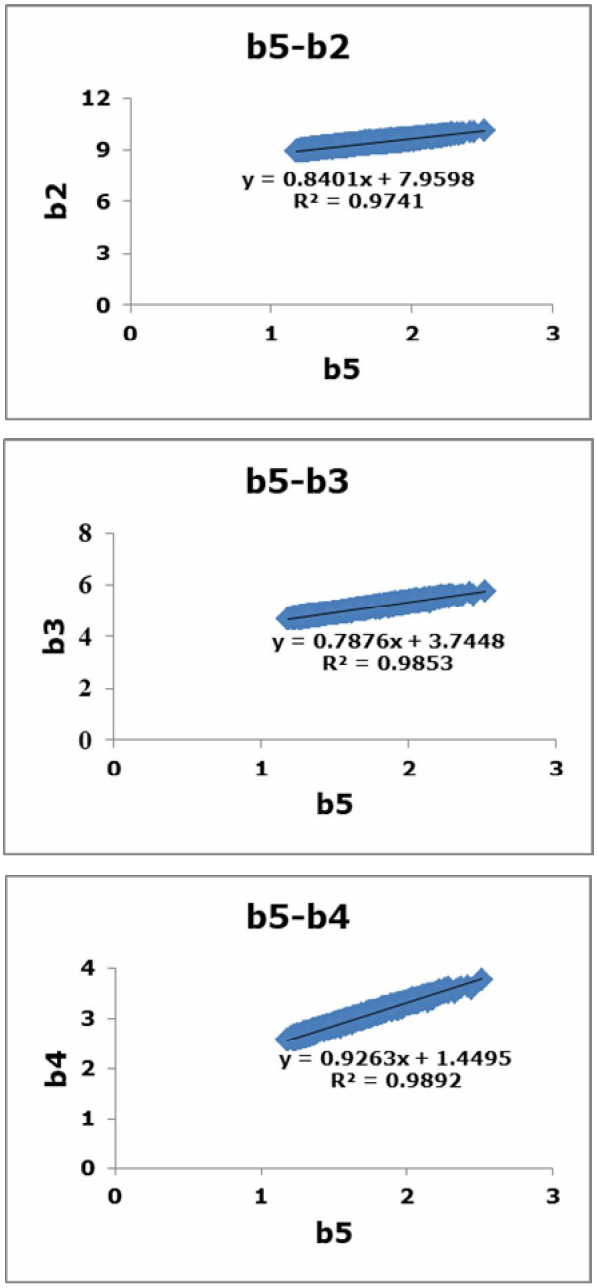

Figure 2. Regression sample *glint* between two bands (band 5 and band 2, band 5 and band 3, band 5 and band 4).

Table 4

Equation *de-glint*

Band	*Slope regression (a)*	*de-glint*
b2	0.8401	b2-(0.8401)*(b5-1.1813)
b3	0.7876	b3-(0.7876)*(b5-1.1813)
b4	0.9263	b4-(0.9263)*(b5-1.1813)

Water column pixel samples used the ROI (Region of Interest) facility, carried out on a point basis (per pixel). Samples taken were sand objects at various depths (for they have a uniform color and are relatively the same) so that they are easily recognized, both in the image and in the field (Suyarso 2019). The relationship between the difference in the depth of the sand object to the normalized channel combination (ln) is shown in the regression graph (Figure 3). The shape of the trend line graph and the R^2 value obtained is good enough for further analysis. The value of R^2 for the Ln(B2)-Ln(B3) pair = 0.9629; R2 pair Ln(B2)-Ln(B4) = 0.9400 and R^2 pair Ln(B3)-Ln(B4) = 0.8561.

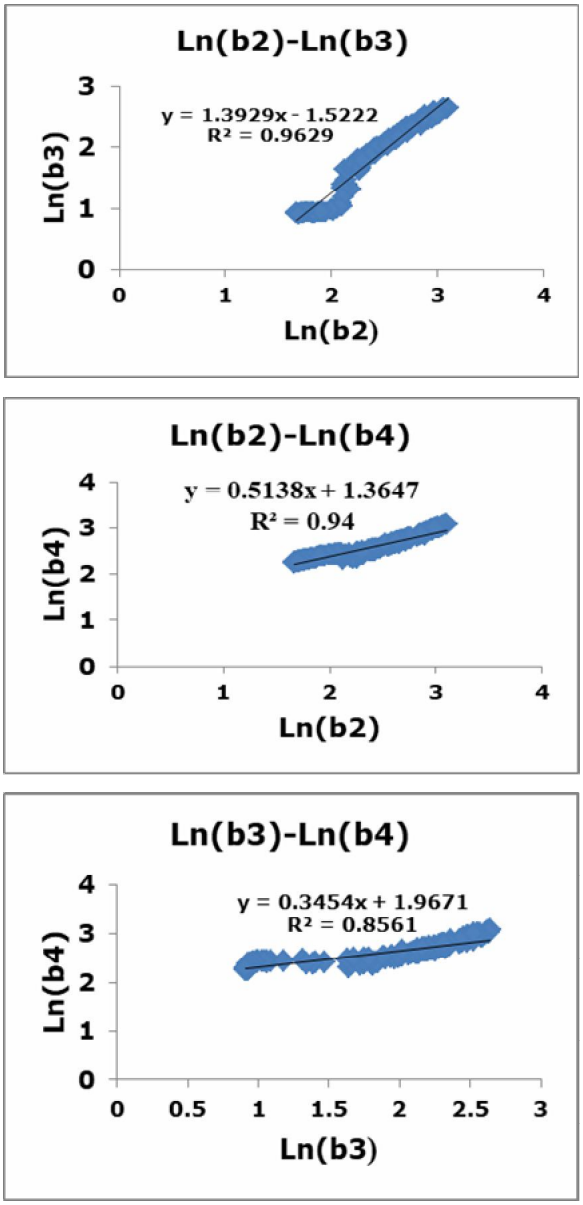

Figure 3. Regression between the two band (Ln) normalized bands collected from sand samples at different depths.

Based on the depth invariant index equation table (Table 5), the results of the water column correction are a new channel which is a combination between channels visible in the Landsat-8 image b4 (red), b3 (green), b2 (blue), namely the blue-green band, blue-red band, and the green-red band. Correlation between band 2 (blue) and band 3 (green) in the depth invariant index equation is applied to improve image quality and obtain information about the basic habitat of shallow sea waters.

Table 5

Invariant index depth equation for water column correction

Band	*Variance*	*Covariance*	*a*	k_i/k_j	*Equation*
Ln(b2)-Ln(b3)	0.19634	0.27198	-0.36637	0.69863	alog(b2)-(0.69863*alog(b3))
Ln(b2)-Ln(b4)	0.39363	0.10033	0.70368	1.92646	alog(b2)-(1.92646*alog(b4))
Ln(b3)-Ln(b4)	0.05514	0.13591	0.25260	2.85540	alog(b3)-(2.85540*alog(b4))

Unsupervised classification using the Iso-Data algorithm was performed to produce 7 classes of pixel grouping and can be used as a base map for field tests (groundtruth). Supervised classification using maximum likelihood classification results in 4 classes (Figure 4). This method works based on probability statistical values so as to minimize unclassified pixels by setting a threshold value as obtained from trial and error to find the optimal value and produce the object class as desired (Richards & Jia 2006; Prayudha 2012).

Groundtruth data from position taking represent 4 types of shallow water base habitat classes as many as 200 points for the validation process, the results of the digital interpretation accuracy test are 10 invalid points so it is said that they cannot be classified and 190 points are valid or can be classified which are divided into 177 samples classified accurate and 13 samples classified as inaccurate. The overall accuracy value obtained is 93.16% with a Kappa coefficient of 0.9056 (Table 6). The limit of the acceptable accuracy value for a shallow water base habitat map is based on SNI 7716: 2011 concerning mapping of seabed habitats shallow, amounting to 60% (Lillesand et al 2008; Congalton & Green 2009).

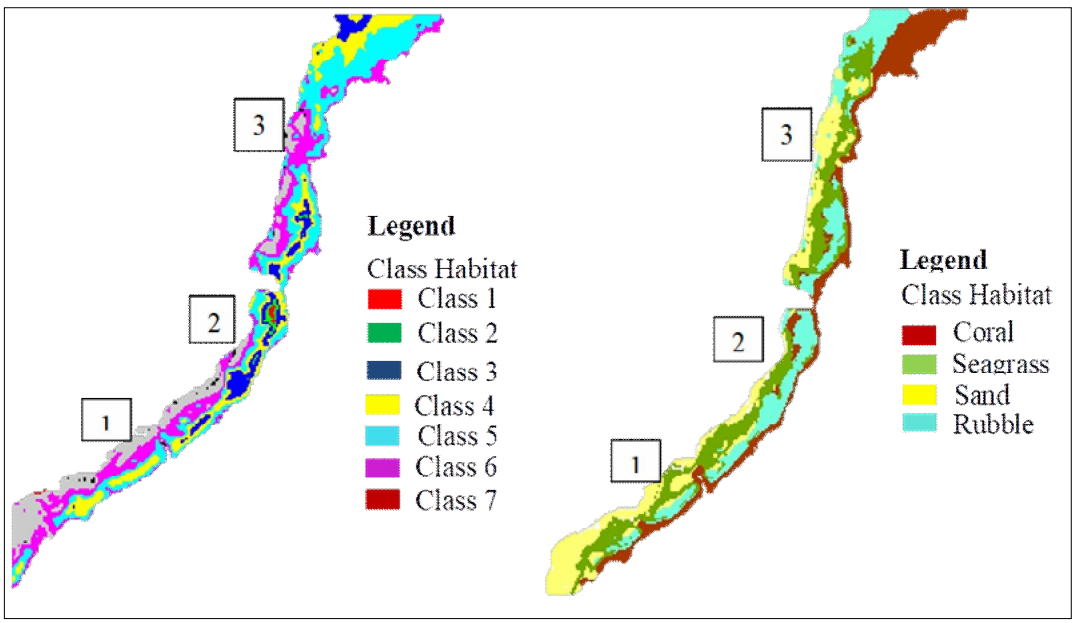

(A) (B)

Figure 4. (A) Habitat map of unsupervised classification, and (B) Habitat map of supervised classification.

Table 6

Accuracy test result based on ground-truthing of parameters

Result classification	Data survey				Total	User's accuracy (%)
	Seagrass	Sand	Rubble	Coral		
Seagrass	64	2	0	0	66	96.97
Sand	2	30	0	0	32	93.75
Rubble	3	0	29	3	35	82.86
Coral	0	2	1	54	57	94.74
Total	69	34	30	57	190	
Producer's accuracy (%)	92.75	88.24	96.67	94.74		
Overall accuracy (%)	93.16					
Kappa coefficient	0.9056					

The distribution of the bottom cover of the waters, namely seagrass, is known through the area value of the object from the classified image analysis results. Based on the interpretation of Landsat 8 imagery data, it is known that the area of seagrass in the waters of Tanjung Merah is 52.81 ha. The result of equation of seagrass cover and seagrass species dominance at each station can be seen in (Table 7). The results of the analysis of seagrass conditions are based on the percentage of seagrass cover according to Rahmawati et al 2014 (Figure 5) that the entire Tanjung Merah waters area generally has seagrass cover which can be categorized as solid cover (51-75%).

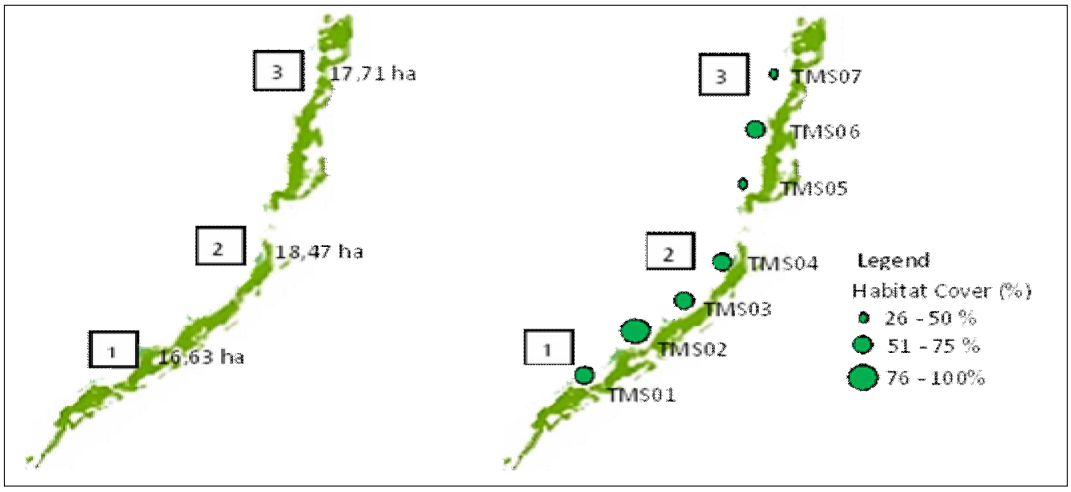

(A) (B)

Figure 5. (A) Distribution map of seagrass, and (B) Condition map of seagrass in Tanjung Merah waters, Bitung City, North Sulawesi (location 1 - RCTI coastal areas; location 2 - Tanjung Merah coastal areas; location 3 - Mayat coastal areas).

Table 7

Precentace of seagrass cover and seagrass species dominance at each station in Tanjung Merah waters

Location	Station	Seagrass cover (%)	Dominance of seagrass species (%)							
			Ea	Th	Cs	Cr	Hu	Hp	Ho	Si
RCTI	TMS01	63.64	19.70	31.82	1.52	3.79	2.27	9.85	7.58	1.52
	TMS02	78.30	21.21	43.18	1.52	2.27	1.52	6.06	4.55	3.03
Mean		70.97	20.45	37.50	1.52	3.03	1.89	7.95	6.06	2.27
Tanjung Merah	TMS03	71.21	18.94	33.59	7.58	9.09	0	13.64	0	0
	TMS04	56.63	18.94	29.69	6.82	9.09	12.12	0	0	0
	TMS05	49.05	31.06	27.27	4.55	2.27	0	0	2.27	0
Mean		58.96	22.98	30.18	6.31	6.82	4.04	4.55	0.76	0
Mayat	TMS06	58.33	29.55	31.82	9.09	2.27	0.00	0.00	3.03	0
	TMS07	33.14	21.97	1.56	16.67	6.06	0.00	0.00	5.30	0
Mean		45.74	25.76	16.69	12.88	4.17	0.00	0.00	4.17	0

Where: Ea = *Enhalus acoroides*; Th = *Thalassia hemprichii*; Cs = *Cymodocea serrulata*; Cr = *Cymodocea rotundata*; Hu = *Halodule uninervis*; Hp = *Halodule pinifolia*; Ho = *Halophila ovalis*; Si = *Syringodium isoetifolium*.

Solid category with the understanding that the diversity of species and the percentage of cover are still relatively high. Change or loss of seagrass beds is generally associated with eutrophication, increased sedimentation, decreased light availability or direct physical disturbance (Erftemeijer & Lewis 2006; Waycott et al 2009; Unsworth et al 2015). These human activities are well-known as threats to seagrass ecosystems (Duffy et al 2018; Zoffoli et al 2020). In addition, the increase in sediment and dissolved sediment is also a factor in the occurrence of high turbidity, causing bad effects for seagrass such as failed to recover or unhealthy seagrass (Duarte et al 2008; Viaroli et al 2008). The increase in population on the coast causes the loss and destruction of seagrass beds in almost all over the world as a result of the impact of human activities so that it significantly reduces the athropogenic impact on coastal ecosystems (Nakamura 2009; Brodie et al 2020).

Conclusions. Mapping of seagrass habitat cover in Tanjung Merah waters using Landsat 8 imagery technique is said to be feasible because of the overall high accuracy results (93.16%), which passed the standards set by SNI 7716 (2011) on Basic Habitat Mapping of Shallow Sea Waters. The extent of seagrass beds in Tanjung Merah waters was determined at 52.81 ha, with the highest coverage at Tanjung Merah Beach (18.47 ha), followed by Mayat Beach (17.71 ha), and RCTI Beach (16.63 ha). It is now established that all areas of Tanjung Merah waters generally have seagrass cover which can be categorized as solid cover (51-75%). It is hoped that concerned management bodies will be able to utilize the findings of this study for purposes of conserving the remaining seagrass habitats in Tanjung Merah coastal waters.

Acknowledgements. The authors would like to extend their deeply gratitude to all those who have helped in conducting research and writing the manuscript.

Conflict of interest. We declare that there is no conflict of interest with any organization regarding material discussed in this manuscript.

References

BIG [Geospatial Information Agency], 2014 Pedoman teknis pengumpulan dan pengolahan data geospasial habitat dasar perairan laut dangkal. Jakarta. [in Indonesian]

Blandon A., zu Ermgassen P. S. E., 2014 Quantitative estimate of commercial fish enhancement by seagrass habitat in southern Australia. Estuarine, Coastal and Shelf Science 141:1-8.

Brodie G., Holland E., N'Yeurt A. D. R., Soapi K., Hills J., 2020 Seagrasses and seagrass habitats in Pacific small island developing states: potential loss of benefits via human disturbance and climate change. Marine Pollution Bulletin 160:111573.

Bujang J. S., Zakaria M. H., Arshad A., 2006 Distribution and significance of seagrass ecosystems in Malaysia. Aquatic Ecosystem Health and Management 9(2):203-214.

Campbell J. B., 1996 Introduction to remote sensing. 2nd edition, Taylor and Francis, London, 622 pp.

Cao K., Batty M., Huang B., Liu Y., Yu L., Chen J., 2011 Spatial multi-objective land use optimization: extensions to the non-dominated sorting genetic algorithm-II. International Journal of Geographical Information Science 25(12):1949-1969.

Congalton R. G., Green K., 2009 Assessing the accuracy of remotely sensed data: principles and practices. Mapping Science Boca Raton, CRC Press, 183 pp.

Duarte C. M., Borum J., Short F. T., Walker D. I., 2008 Seagrass ecosystems: their global status and prospects. In: Aquatic ecosystems: trends and global prospects. Polunin N. V. C. (ed), Cambridge University Press, pp. 281-294.

Duffy J. P., Pratt L., Anderson K., Land P. E., Shutler J. D., 2018 Spatial assessment of intertidal seagrass meadows using optical imaging systems and a lightweight drone. Estuarine, Coastal and Shelf Science 200:169-180.

Erftemeijer P. L. A., Lewis R. R. R., 2006 Environmental impacts of dredging on seagrasses: a review. Marine Pollution Bulletin 52(12):1553-1572.
Fonseca M., Whitfield P. E., Kelly N. M., Bell S. S., 2002 Modeling seagrass landscape pattern and associated ecological attributes. Ecological Applications 12(1):218-237.
Giardino C., Brando V. E., Gege P., Pinnel N., Hochberg E., Knaeps E., Reusen I., Doerffer R., Bresciani M., Braga F., Foerster S., Champollion N., Dekker A., 2019 Imaging spectrometry of inland and coastal waters: state-of-the-art, achievements and perspectives. Survey in Geophysics 40:401-429.
Green E. P., Short F. T., 2003 World atlas of seagrasses. Prepared by the UNEP World Conservation Monitoring Centre. University of California Press, Berkeley, CA, USA, 298 pp.
Hedley J. D., Harbone A. R., Mumby P. J., 2005 Simple and robust removal of sun glint for mapping shallow-water benthos. International Journal of Remote Sensing 26(10):2107-2112.
Hossain M. S., Bujang J. S., Zakaria, M. H., Hashim M., 2015 The application of remote sensing to seagrass ecosystems: an overview and future research prospects. International Journal of Remote Sensing 36(1):61-114.
Kustiyo, Hayati A. K., 2016 Haze removal in the visible bands of Landsat 8 OLI over shallow water area. International Journal of Remote Sensing and Earth Sciences 13(2):151-157.
Lillesand T., Kiefer R. W., Chipman J., 2008 Remote sensing and image interpretation. 6th edition, John Wiley and Sons, Inc., 704 pp.
Lyzenga D. R., 1978 Passive remote sensing techniques for mapping water depth and bottom features. Applied Optics 17(3):379-383.
Lotze H. K., Lenihan H. S., Bourque B. J., Bradbury R. H., Cooke R. G., Kay M. C., Kidwell S. M., Kirby M. X., Peterson C. H., Jackson J. B. C., 2006 Depletion, degradation, and recovery potential of estuaries and coastal seas. Science 312:1806-1809.
Nakamura Y., 2009 Status of seagrass ecosystem in the Kuroshio region: seagrass decline and challenges for future conservation. Kuroshio Science 3(1):39-44.
Orth R. J., Carruthers T. J. B., Dennison W. C., Duarte C. M., Fourqurean J. W., Heck K. L. Jr., Hughes A. R., Kendrick G. A., Kenworthy W. J., Olyarnik S., Short F. T., Waycott M., Williams S. L., 2006 A global crisis for seagrass ecosystems. BioScience 56(12):987-996.
Prayudha B., 2012 Pemetaan sumberdaya kepesisiran melalui teknologi penginderaan jauh di perairan Ternate, Tidore dan sekitarnya. Dalam: Eksosistem pesisir Ternate, Tidore dan sekitarnya, Provinsi Maluku Utara] (Giyanto, edition). Coremap, P2O-LIPI, Jakarta, pp. 7-18. [in Indonesian]
Rahmawati S., Indarto H., Azkab M. H., Kiswara W., 2014 Panduan monitoring padang lamun. Pusat Penelitian Oseanografi LIPI, Jakarta, 34 pp. [in Indonesian]
Richards J. A., Jia X., 2006 Remote sensing digital image analysis. Springer, Berlin, 439 pp.
SNI [Indonesian Nasional Standard], 2011 Standar Nasional Indonesia Nomor 7716 Tentang Pemetaan Habitat Dasar Perairan Laut Dangkal. [in Indonesian]
Suyarso, 2019 Teknik eksplorasi sumber daya pesisir (terumbu karang dan mangrove) berbasis geospasial. Penerbit ANDI, Yogyakarta, 266 pp. [in Indonesian]
Topouzelis K., Makri D., Stoupas N., Papakonstantinou A., Katsanevakis S., 2018 Seagrass mapping in Greek territorial waters using Landsat-8 satellite images. International Journal of Applied Earth Observation and Geoinformation 67:98-113.
Unsworth R. K. F., Collier C. J., Waycott M., McKenzie L. J., Cullen-Unsworth L. C., 2015 A framework for the resilience of seagrass ecosystems. Marine Pollution Bulletin 100(1):34-46.
USGS [United States Geological Survey], 2015 Landsat 8 (L8) Data Users, Handbook Version 1.0. EROS Sioux Falls, South Dakota.
USGS [United States Geological Survey], 2016 Landsat 8 (L8) Data Users Handbook, LSDS-1574 Version 2.0.

Veettil B. K., Ward R. D., Lima M. A. C., Stankovitch M., Ngoc H. P., Quang N. X., 2020 Opportunities for seagrass research derived from remote sensing: a review of current methods. Ecological Indicators 117:1-21.
Viaroli P., Bartoli M., Giordani G., Naldi M., Orfanidis S., Zaldivar J. M., 2008 Community shifts, alternative stable states, biogeochemical controls and feedbacks in eutrophic coastal lagoons: a brief overview. Aquatic Conservation: Marine and Freshwater Ecosystems 18(1):105-117.
Waycott M., Duarte C. M., Carruthers T. J. B., Orth R. J., Dennison W. C., Olyarnik S., Calladine A., Fourqurean J. W., Heck K. L., Hughes A. R., Kendrick G. A., Kenworthy W. J., Short F. T., Williams, S. L., 2009 Accelerating loss of seagrass across the globe threatens coastal ecosystems. Proceedings of the National Academy of Sciences of the USA 106:12377-12381.
Zoffoli M. L., Gernez P., Rosa P., Le Bris A., Brando V. E., Barillé A. L., Harin N., Peters S., Poser K., Spaias L., Peralta G., Barillé L., 2020 Sentinel-2 remote sensing of *Zostera noltei*-dominated intertidal seagrass meadows. Remote Sensing of Environment 251:112020.

Received: 12 March 2021. Accepted: 19 April 2021. Published online: 28 April 2021.
Authors:
Jesica Olivia Patty, Postgraduate Aquatic Science Study Program, Faculty of Fisheries and Marine Science, Sam Ratulangi University, Manado, 95115, Indonesia, e-mail: jesicaolivia1996@gmail.com
Billy Theodorus Wagey, Marine Science Study Program, Faculty of Fisheries and Marine Science, Sam Ratulangi University, Manado, 95115, Indonesia, e-mail: billywagey@unsrat.ac.id
Ferdinand Frans Tilaar, Aquatic Resource Management Study Program, Faculty of Fisheries and Marine Science, Sam Ratulangi University, Manado, 95115, Indonesia, e-mail: ftilaar2135@gmail.com
Lawrence J. L. Lumingas, Aquatic Resource Management Study Program, Faculty of Fisheries and Marine Science, Sam Ratulangi University, Manado, 95115, Indonesia, e-mail: ljllumingas@unsrat.ac.id
Calvyn Sondak, Marine Science Study Program, Faculty of Fisheries and Marine Science, Sam Ratulangi University, Manado, 95115, Indonesia, e-mail: calvyn_sondak@unsrat.ac.id
Suzanne Undap, Aquaculture Study Program, Faculty of Fisheries and Marine Science, Sam Ratulangi University, Manado, 95115, Indonesia, e-mail: suzanneundap@unsrat.ac.id
Deiske Sumilat, Marine Science Study Program, Faculty of Fisheries and Marine Science, Sam Ratulangi University, Manado, 95115, Indonesia, e-mail: deiske.sumilat@gmail.com

How to cite this article:
Patty J. O., Wagey B. T., Tilaar F. F., Lumingas L. J. L., Sondakh C. F. A., Undap Z., Sumilat D., 2021 Seagrass mapping using Landsat-8 satellite images in Tanjung Merah waters, Bitung City, North Sulawesi. AES Bioflux 13(1):37-47.